

ANALYSIS OF WIND DRIVEN SELF EXCITED INDUCTION GENERATOR CONNECTED TO GRID INTERFACE WITH MULTI LEVEL INVERTER

SWATI DEVABHAKTUNI

Associate Professor, Gokaraju rangaraju institute of engineering and technology,
Hyderabad, Andhra Pradesh, India
swatikjm@gmail.com

S.V.JAYARAM KUMAR

Professor, Jawaharlal Nehru Technological University,
Hyderabad, Andhra Pradesh,
svjkumar101@rediffmail.com

Abstract

This paper presents an investigation of multi level inverter of 27 levels used along with the voltage source rectifier unit as an interface between Self excited induction generator and grid. Making use of multi level inverter benefits of low harmonics distortion reduced number of switches and reduced switching losses results in improvement of the p.f at grid, to compensate the reactive power and to suppress the total harmonic reduction. The generated voltage of the wind driven self excited induction generator mainly depends on the wind velocity, appropriate excitation capacitance and grid conditions. The main objective of this paper is to track the maximum power of the grid connected SEIG driven by wind turbine. In previous literature there is no discussion about the grid connected SEIG interface with the AC/DC link through the multi level of 27 levels. The variable magnitude, variable frequency, voltage of the generator can be controlled by the proper modulation index. The modulation index of the proposed multi level inverter is adjusted to obtain the maximum output power. The results are valid through MATLAB/SIMULINK software.

Keywords: Self excited induction generator (SEIG), Wind turbine, Hybrid nine level inverter, voltage source rectifier, grid.

1. Introduction

Wind energy conversion scheme using a wind turbine driven SEIG, modern power electronic converter have been modeled, analyzed and implemented. The wind turbine generator system is producing an electricity from wind is the fastest growing energy technology in the world. Modern variable frequency drives operate by converting a 3 ϕ voltage source to DC using uncontrolled rectifier. The minimum and maximum values of capacitance required for self excitation have been analyzed previously [5] – [7]. Especially in remote areas, Self-Excited Induction Generators are producing good electricity

compared other generators. By using an advanced power electronic converters, the variable voltage variable frequency of the SEIG is converted into constant voltage and constant frequency. The squirrel cage induction generators have robust construction, lower inertia, and run-time cost, less maintenance cost and better transient performance. The generated voltage of the SEIG is mainly depends upon the excitation capacitance values, change in wind velocity and load conditions. The reactive power requirement by the induction generator can also be supplied by a group of capacitors. If the capacitance is insufficient, the induction generators will not build up

voltage. The main draw of the induction generator is need of reactive to build up the terminal voltage.

2. System Configuration

A proposed ZSI based wind driven SEIG fed load is shown in Figure 1. The wind power generation system consisting of a wind turbine driven SEIG connected to the grid through an impedance source inverter. The power conversion efficiency of ZSI is improved compared to the traditional inverters for wind electric power generation. In traditional inverters, the upper and lower switches of each phase cannot be switched on simultaneously either by EMI noise. The output voltage of the ZSI is limited to either greater or lesser than the given input voltage. The variable output voltage from the induction generator is rectified and then inverted by using the proposed inverter. The ZSI can produce an output voltage greater than the input voltage by controlling the shoot through time T_0 . This proposed scheme is used to improve the power factor and reduce harmonic current. The parameters used in the SEIG can be obtained by conducting no load test and short circuit test on the induction generator when it is used as an induction motor. The traditional tests used to determine the parameters are the open circuit test and the short circuit test. The induction machine used as the SEIG in this investigation is a three-phase wound rotor induction motor with specification: 415V, 7.5A, 3.7kW, 50Hz, and 4 poles.

The proposed system is as shown in Fig.1

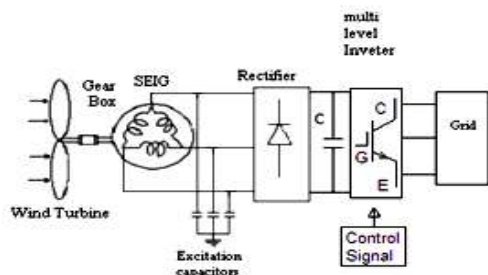


Fig.1.Overall system description

2.1. Self excited induction generator modeling

To find the decoupling signal given in Fig. 1 some of the equations of an induction machine in the excitation reference frame are considered[5]. Since in the stator oriented reference frame all variables are expressed in a reference frame oriented to the stator flux linkage space vector, a mathematical model needs to be developed to find the relationship between the stator flux linkage and the stator currents

$$\lambda_{ds}^e = L_s i_{ds}^e + L_m i_{dr}^e \quad (1)$$

$$\lambda_{dr}^e = L_m i_{ds}^e + L_r i_{dr}^e \quad (2)$$

$$\lambda_{qs}^e = L_s i_{qs}^e + L_m i_{qr}^e \quad (3)$$

$$\lambda_{qr}^e = L_m i_{qs}^e + L_r i_{qr}^e \quad (4)$$

$$0 = R_r i_{dr}^e + p \lambda_{dr}^e - (\omega_e - \omega_r) \lambda_{qr}^e \quad (5)$$

$$0 = R_r i_{qr}^e + p \lambda_{qr}^e - (\omega_e - \omega_r) \lambda_{dr}^e \quad (6)$$

From equations (1) and (2)

$$\lambda_{dr}^e = \frac{L_r}{L_m} (\lambda_{ds}^e - \sigma L_s i_{ds}^e) \quad (7)$$

And from equation (3) and (4)

$$\lambda_{qr}^e = \frac{L_r}{L_m} (\lambda_{qs}^e - \sigma L_s i_{qs}^e) \quad (8)$$

Where

$$\sigma = 1 - \frac{L_m^2}{L_r L_s} \quad (9)$$

From the equations (1) and (2) the rotor currents can be expressed as

$$i_{dr}^e = \frac{\lambda_{ds}^e - L_s i_{ds}^e}{L_m} \quad (10)$$

$$i_{qr}^e = \frac{\lambda_{qs}^e - L_s i_{qs}^e}{L_m} \quad (11)$$

The frequency of the generated voltage is estimated as :

$$\omega_e = \frac{(V_{qs} - i_{qs} R_s) \lambda_{ds} - (V_{ds} - i_{ds} R_s) \lambda_{qs}}{\lambda_{qs}^2 + \lambda_{ds}^2} \quad (12)$$

3. Design of Bridge Rectifier

The design and operation of six and twelve pulse bridge rectifier are explained in this section.

3.1. Operation of Six Pulse Bridge Rectifier

One of the most common circuits used in power electronics is the 3-phase line

commutated 6-pulse rectifier bridge, which comprises 6 diodes in a bridge connection. Single-phase bridges will not be covered here because their operation can be deduced as a simplification of the 3-phase bridge. In the diode bridge, the diodes are not controlled from an external control circuit. Instead, commutation is initiated externally by the changes that take place in the supply line voltages, hence the name line commutated rectifier as shown in fig.2. According to convention, the diodes are labeled D1 to D6 in the sequence in which they are turned ON and OFF. This sequence follows the sequence of the supply line voltages.

The 3-phase supply voltages comprise 3 sinusoidal voltage waveforms 120° apart which rise to their maximum value in the sequence A – B – C. According to convention, the phase-to-neutral voltages are labeled V_A , V_B and V_C and the phase-to-phase voltages are V_{AB} , V_{BC} and V_{CA} , as shown in fig.3. These voltages are usually shown graphically as a vector diagram, which rotates counter-clockwise at a frequency of 50 times per second. A vector diagram of these voltages and their relative positions and magnitudes is shown below. The sinusoidal voltage waveforms of the supply voltage may be derived from the rotation of the vector diagram.

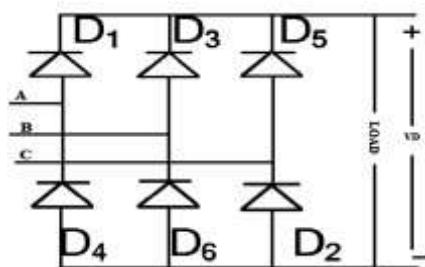


Fig.2 three phase diode rectifier

The bridge comprises two commutation groups, one connected to the positive leg, consisting of diodes D1–D3–D5, and one connected to the negative leg, consisting of diodes D4–D6–D2. The commutation transfers the current from one diode to

another sequence and each diode conducts current for 120° of each cycle as shown in Figure 3. The commutation transfers the current from one diode to another in sequence and each diode conducts current for 120° of each cycle as shown in Figure 3. In the upper group, the positive DC terminal follows the highest voltage in the sequence $V_A-V_B-V_C$ via diodes D1–D3–D5. When V_A is near its positive peak, diode D1 conducts and the voltage of the +DC terminal follows V_A . The DC current flows through the load and returns via one of the lower group diodes. With the passage of time, V_A reaches its sinusoidal peak and starts to decline. At the same time, V_B is rising and eventually reaches a point when it becomes equal to and starts to exceed V_A . At this point, the forward voltage across diode D3 becomes positive and it starts to turn on. The commutating voltage in this circuit, V_B-V_A starts to drive an increasing commutation current through the circuit inductances and the current through D3 start to increase as the current in D1 decreases. In a sequence of events similar to that described above, commutation takes place and the current is transferred from diode D1 to diode D3. At the end of the commutation period, diode D1 is blocking and the +DC terminal follows V_B until the next commutation takes place to transfer the current to diode D5. After diode D5, the commutation transfers the current back to D1 and the cycle is repeated.

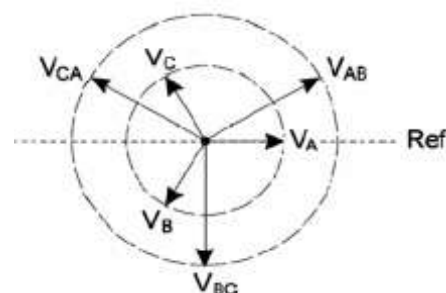


Fig.3 vector diagram of the 3-phase main supply voltages

In the lower group, a very similar sequence of events takes place, but with negative voltages and the current flowing

from the load back to the mains. Initially, D2 is assumed to be conducting when V_C is more negative than V_A . As time progresses, V_A becomes equal to V_C and then becomes more negative. Commutation takes place and the current is transferred from diode D2 to D4. Diode D2 turns off and D4 turns on. The current is later transferred to diode D6, then back to D2 and the cycle is repeated. In Figure 4, the conducting periods of the diodes in the upper and lower groups are shown over several cycles of the 3-Phase supply. This shows that only 2 diodes conduct Current at any time (except during the commutation period, which is assumed to be infinitely short) and that each of the 6 diodes conducts for only one portion of the cycle in a regular sequence. The commutation takes place alternatively in the top group and the bottom group. The DC output voltage V_D is not a smooth voltage and consists of portions of the phase-to-phase voltage waveforms. For every cycle of the 50 Hz AC waveform (20 msec), the DC voltage V_D comprises portions of the 6 voltage pulses, $V_{AB}, V_{AC}, V_{BC}, V_{BA}, V_{CA}, V_{CB}$, etc, hence the name 6-pulse rectifier bridge.

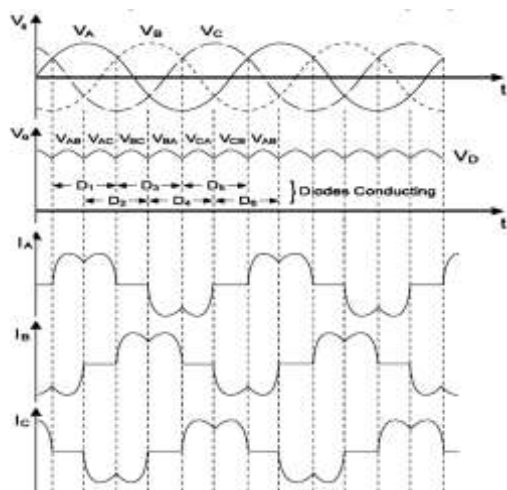


Fig.4. Out put results of 6-pulse ode rectifier

As fig.8 the average magnitude of the DC voltage may be calculated from the voltage Waveform shown above. The average value is obtained by integrating the voltage over one of the repeating 120° portions of

the DC voltage curve.

The average value of the dc voltage can be calculated by

$$V_d = \left[\frac{3\sqrt{2}}{\pi} \right] \left[\frac{\sqrt{3}}{\sqrt{2}} \right] * V_{dc} * \eta_i \quad (13)$$

4. The VSI operation

The dump load connected to the VSI DC side will be controlled so that the voltage across the C_{DC} capacitor remains at a constant level, maintaining the system voltage in a standard variation range. Thus, the difference between the power delivered by the IG and the loads demand will circulate through the VSI towards the CDC capacitor, which acts as a short-time energy storage element. This leads to a voltage increase on the DC capacitor. The DC voltage variation ratio depends on the capacitance value and on the amount of power transferred from the IG towards the capacitor. The capacitor value plays a very important role during transitory regimes, when it has to handle large amounts of energy (in or out). Large capacitors ensure low voltage drops across the IG lines when dynamic loads (as induction motors) are connected to the system [5]. Likewise, for unbalanced loads asymmetrical currents will flow through the inverter lines, producing voltage variations on the CDC capacitor. Thereby, the voltage variation on the CDC capacitor has two sources: the first-one is the exceeding active power from the IG, which is dissipated in the dump load, and the second-one is the reactive power flow through the inverter for asymmetrical and harmonics currents flow. For symmetrical three-phase reactive currents, the voltage variation on the CDC capacitor is close to zero. Two controllers are used to regulate the system voltage: a PI controller and an on/off controller, as shown in fig. 5. The PI controller is the leading voltage regulator. It compensates the voltage drops across the inverter arms and filter, IG leakage impedances, and other circuit elements, which usually led to a decrease of the IG voltage. The IG root-mean-square (RMS) voltage (V_{AB}) is the

feedback signal, it is compared with the 230 V reference signal (V_{REF}), and the error feeds the PI controller, giving the reference signal (V_{DCref}) for the second controller. The on-off controller is used to maintain constant the CDC voltage. The allowed voltage variation (ripple) across CDC capacitor (EVDC) will give the frequency and the width of the pulses that drive the Td transistor from the dump load.

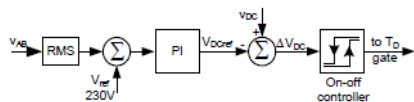


Fig.5. The DC capacitor voltage regulation

5. Results and Discussions

The simulation was carried out using MATLAB/SIMULINK. The features in the Power Systems Blockset are used to model an inverter, rectifier and all circuit components. The comparison is made between self excited induction generator connected to the grid interface through the nine level and 27 level inverter.

The MATLAB/Simulink model is as shown in Fig.6.

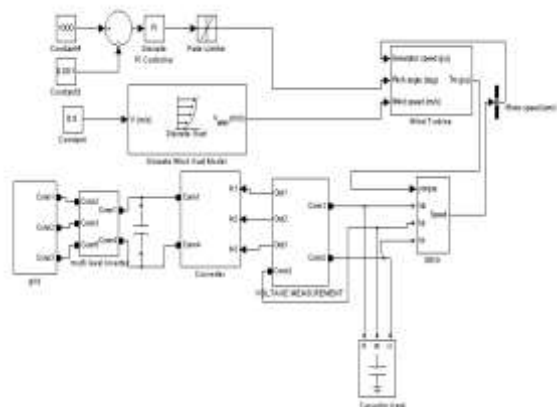
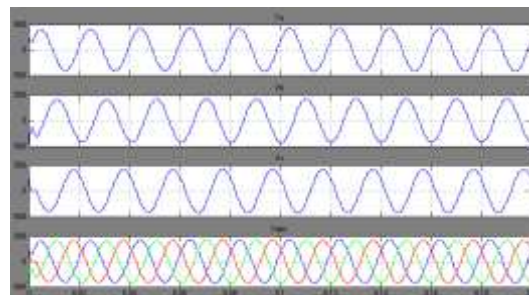


Fig.6. Simulink model of SEIG fed MLI with grid
Here, transient waveforms of the generator voltage (V_{abc}), generator current (I_{abc}), Speed of the generator, Electromagnetic torque, rectifier current, voltage at capacitor, inverter voltage, grid voltage, grid current are given under the sudden application and short circuit at grid for conventional six pulse rectifier is as shown in Fig.7 respectively. The Simulink model

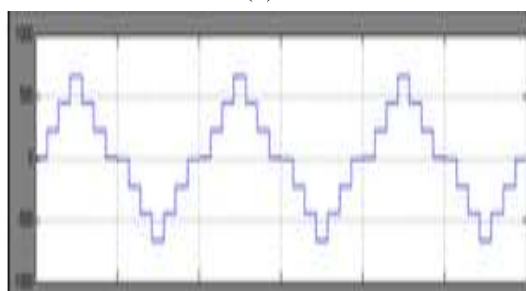
for the nine level inverter fed SEIG is as shown in Fig.8.

The Simulink model for the nine level inverter fed SEIG is as shown in Fig.10.

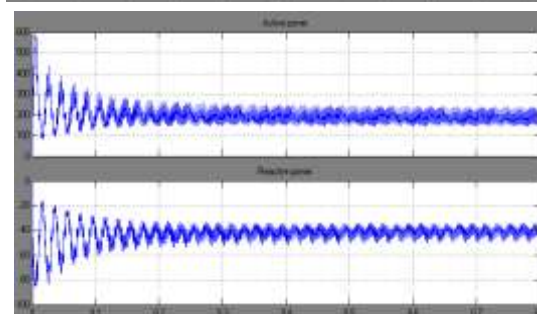
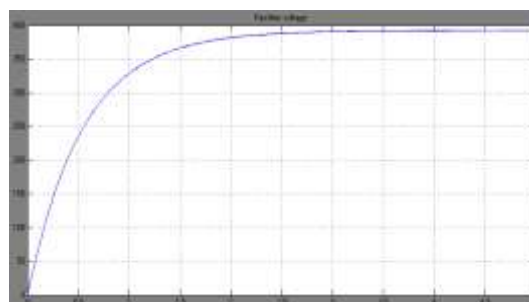
(a)



(b)



(c)



(d)

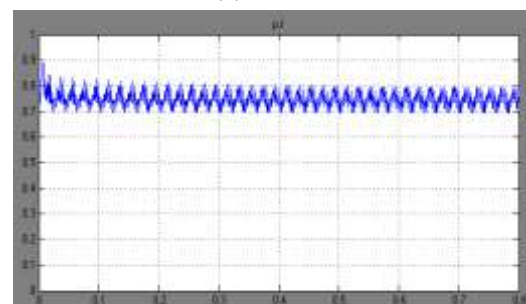
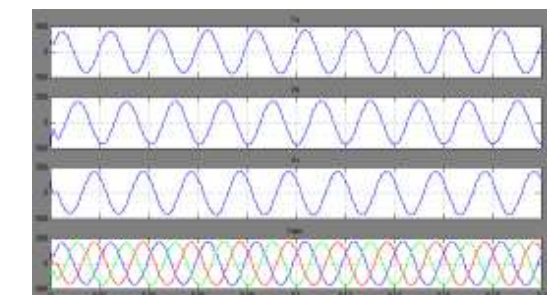
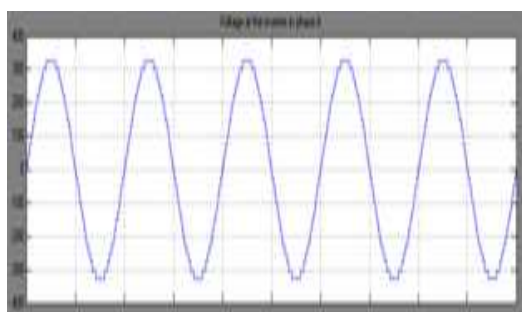


Fig.7.For nine level inverter(a).Generated voltage
(b)Inverter voltage (c).D.C.voltage
(d).Active and reactive power at the grid
(e) p.f at the grid

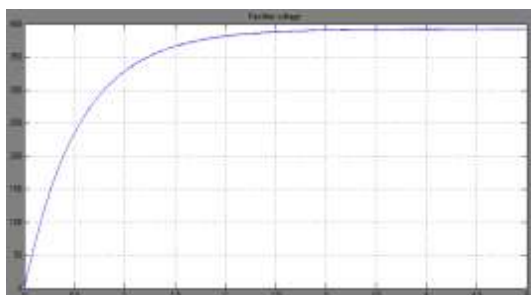


(e) p.f at the grid

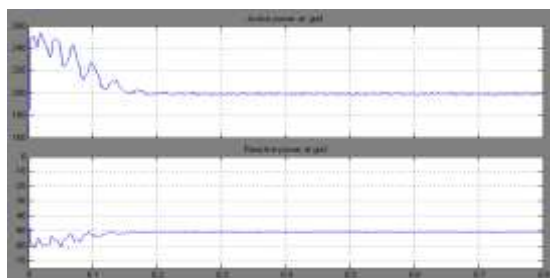
(a)



(b)



(c)



(d)



(e)

Fig.8.For 27 level inverter(a).Generated voltage
(b)Inverter voltage (c).D.C.voltage
(d).Active and reactive power at the grid
(e) p.f at the grid

6. Conclusion

The modeling and simulation analysis of wind driven SEIG with 27 level inverter, results are tested with the grid. The SEIG in its no load condition generated a phase voltage of 390 V at a speed of 1650 rpm. For a wind velocity of 6.5 m/s, the proposed inverter produced an output voltage of 390 V were obtained for grid connected SEIG driven by wind turbine. The required output voltage and active, reactive powers were obtained for a wind velocity range of 6.5m/s. From the simulation it is confirmed that as the number of levels are increased at the inverter the harmonics are also reduced. The output voltage is controlled to give a constant voltage by D.C/A.C link .With the use of the multilevel inverter there is an improvement in the p.f. The ripples in the p.f are eliminated. But as the number of levels are increased the it was becoming difficulty to supply pulses to the inverter and the switching losses are increased. The performance characteristics of the wind turbine SEIG are improved due to the increase in the number of levels at the inverter and hence results in improved load performance.

Appendix

1. Machine Parameters

The parameters of the 3.5 kW,440V, 7.5A, 50 Hz,4-pole induction machine are given below.

$$R_s = 0.69 \Omega, R_r = 0.74\Omega, L_{ls} = L_{lr} = 1.1 \text{ mH}, J = 0.23\text{kg/m}^2,$$

$$L_{ss} = L_{ls} + L_m \text{ and } L_{rr} = L_{lr} + L_m.$$

- Excitation capacitor $C = 15 \mu\text{F}$ / phase and Capacitor at rectifier $C=3200 \mu\text{F}$

3. Air gap voltage:

The piecewise linearization of

magnetization characteristic of machine is given by:

$$\begin{aligned} E_1 &= 0 & X_m &\geq 260 \\ E_1 &= 1632.58 - 6.2X_m & 233.2 &\leq X_m \leq 260 \\ E_1 &= 1314.98 - 4.8X_m & 214.6 &\leq X_m \leq 233.2 \\ E_1 &= 1183.11 - 4.22X_m & 206 &\leq X_m \leq 214.6 \\ E_1 &= 1120.4 - 3.9.2X_m & 203.5 &\leq X_m \leq 206 \\ E_1 &= 557.65 - 1.144X_m & 197.3 &\leq X_m \leq 203.5 \\ E_1 &= 320.56 - 0.578X_m & X_m &\leq 197.3 \end{aligned}$$

References

- [1] O. Ojo, O. Omozusi, and A. A. Jimoh, "The operation of an inverter assisted single phase induction generator," IEEE Trans. Ind. Electron., vol. 47, no. 3, pp. 632–640, Jun.2000.
- [2] D. Henderson, "An advanced electronic load governor for control of micro hydroelectric generation," IEEE Trans. Energy Converse., vol. 13, no. 3, pp. 300–304, Sep. 1998.
- [3] IEEE Guide for Harmonic Control and Reactive Compensation of Static Power Converters, IEEE Standard 519-1992.
- [4] R. Bonert and S. Rajakaruna, "Self-excited induction generator with excellent voltage and frequency control," Proc. Inst. Electr. Eng. Gener. Transm. Distrib., vol. 145, no. 1,
- [5] Malik, N.H., and Al-Bahrani, A.H., "Influence of the Terminal Capacitor on the Performance Characteristics of a Self-Excited Induction Generator ", IEE Proc C., Vol. 137, No. 2, March 1990, pp. 168-173.
- [6] Nandakumar, V.N, Yadukumar, K., Sureshkumar, T., Ragupathi, S., and Hegde, R.K., "A WindDriven Self-Excited Induction Generator With Terminal Voltage Controller and Protection Circuits", IEEE Power Conversion Conference, 1993, pp. 484-489.
- [7] Bonert, R., and Rajakaruna, R., "Self-Excited Induction Generator with Excellent Voltage and Frequency Control", IEE Proc.-Gener

Transm. Distrib., Vol.145, No.1, January 1998, pp.33-39.

- [8] Mitronikas, E.D., Safacas, A.N. and Tatakis, E.C., "A new stator resistance tuning method for statorflux- oriented vector-controlled induction motor drive", IEEE Transactions on Industrial Electronics, Vol. 48 Issue: 6, Dec. 2001, pp. 1148 –1157.